Polym. Bull. (2009) 63:565–573
DOI 10.1007/s00289-009-0128-x

Isothermal crystallization kinetics of AB_3 hyperbranched polymer (HBP)/polypropylene (PP) blends

Guangtian Liu · Minshou Zhao

Received: 8 January 2009 / Revised: 7 May 2009 / Accepted: 22 June 2009 /

Abstract In this paper, the isothermal crystallization kinetics of pure isotactic polypropylene (iPP) and iPP with 5% AB_3 hyperbranched polymer (HBP) added had been investigated by differential scanning calorimetry (DSC). During isothermal crystallization, the crystallization rate of the blends was higher than those of iPP remarkably. Moreover, the value of $t_{1/2}$ became smaller with increasing the HBP molecular weight in blends, however, the crystallization rate of the blend decreased when the higher molecular weight HBP ($\bar{M}_n = 12{,}500$) was added. The crystallization rate of the blends was more sensitive to temperature than that of iPP. An increase in the Avrami exponent may be attributed to the fractal structure of hyperbranched polymer.

Keywords Crystallization kinetics · Hyperbranched polymer (HBP) · Polypropylene · Blend

Introduction

In the past decades, hyperbranched polymers had attracted considerable attention due to their remarkable properties such as reduction of melt and solution viscosity, high solubility and ready to be functional in comparison to their linear analogues [1–3]. In recent years, many functional hyperbranched polymers with various terminal groups, such as hydroxyl, carboxyl, acetoxy, and vinyl etc., had been investigated as additives [4], catalysis [5], rheology modifiers [6], blend components [7] and so forth. The effect of adding hyperbranched polyester-amide to PP was investigated, and indeed it was found that the dyeability of PP fibers was highly

---

G. Liu (✉) · M. Zhao
Institute of Environmental and Chemistry Engineering, Yanshan University, 066004 Qinhuangdao, Heibei Province, People’s Republic of China
e-mail: gtldesire@163.com

improved without affecting other properties of the material [8]. It had been known that the physical properties of polymeric materials strongly depended on their microstructure and crystallinity, however, there were not much work about the crystallization behavior of hyperbranched polymer (HBP)/PP blend. In this paper, the isothermal crystallization kinetics of pure isotactic polypropylene (iPP) and iPP with 5% AB_3 hyperbranched polymer (HBP) added was investigated using differential scanning calorimetry (DSC). Moreover, the reasons were also discussed about the differences in crystallization behaviors between pure iPP and iPP with 5% HBP added. This study would be useful for designing the processing parameters and obtaining the relation between crystallization behavior and the final mechanical properties of the blends.

Experimental part

Materials

Commercial i-PP (PPH-XD-425, MFR = 47.6 g/10 min) was provided by Jinjiang Petrochemical Co. Ltd. (Jilin, China); the different molecular weight AB_3 HBP samples ($\bar{M}_n = 7{,}800, \bar{M}_n = 10{,}820, \bar{M}_n = 12{,}500$) were self-prepared [9], and the Schematic structures were showed in Fig. 1; the HBP was blended with iPP in a single-screw extruder (type XJ-20, Scientific Research Instrument Factory, Jilin University, Jilin, China). Before being extruded, HBP and iPP were dried at 80 °C for 4 h. The mixtures of HBP and iPP were extruded at 180–190 °C under a screw rotating speed of 20 rpm. The extruded samples were cooled and then granulated.

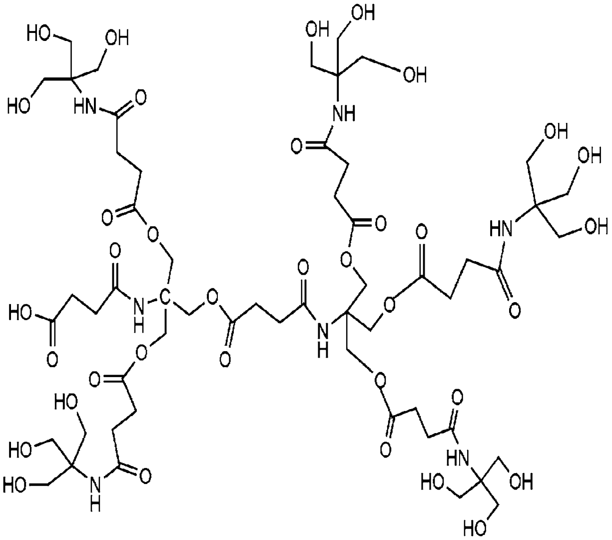

Fig. 1 The Schematic structures of AB_3 hyperbranched poly (amide-ester) (HBP)

Isothermal crystallization kinetics

The crystallization behaviors were investigated by using a Perkin-Elmer DSC-7 thermal analyzer. Before data gathering, all samples were heated to 200 °C and held in the molten state for 5 min to eliminate the influence of thermal history. All operations were carried out under a nitrogen environment. Samples' weights were about 7 mg. In isothermal crystallization experiments, the sample melts were subsequently quenched to the crystallization temperatures at a rate of 40 °C/min. The exotherms were recorded at selected crystallization temperatures: 118, 122, 126, and 130 °C, respectively.

The morphologies

The morphologies of the blends on thin films were studied by using an optical polarizing microscope (type 59-XA, Yongheng Optical Instrument company, shanghai, China) with a Mettler FP-90 automatic hot-stage thermal controller. The samples were sandwiched between microscope cover slips, melted at 200 °C for 5 min in a separate hot stage, and then rapidly moved to another hot stage which was equipped with the microscope and which was set to the crystallization temperature (130 °C).

Results and discussion

The isothermal crystallization kinetics of a material can be analyzed by evaluating its degree of crystalline conversion as a function of time at a constant temperature. The variation of the crystallinity is related to the ratio of the heat generated at time t to the heat generated at infinite time according to the equation [10, 11]

$$X(t) = {}^{Q_t}\!/_{Q_\infty} = \int_0^t (\mathrm{d}H/\mathrm{d}t)\mathrm{d}t \Big/ \int_0^\infty (\mathrm{d}H/\mathrm{d}t)\mathrm{d}t \tag{1}$$

where d*H*/d*t* is the rate of heat evolution. Development of relative crystallinity can be analyzed using the Avrami equation [12–14]

$$X(t) = 1 - \exp(-k_n t^n) \tag{2}$$

where n is a constant whose value depends on the mechanism of nucleation and on the form of crystal growth, $X(t)$ is the relative crystallinity at time t, k_n is a constant containing the nucleation and the growth parameters. The crystallization half-time, $t_{1/2}$, defined as the time to a relative crystallinity of 50%, can be obtained:

$$t_{1/2} = \left(\frac{\ln 2}{k_n}\right)^{1/n} \tag{3}$$

This Eq. 2 can be changed to

$$\ln(1 - X(t)) = -k_n t^n \tag{4}$$

$$\lg[-\ln(1 - X(t))] = n \lg t + \lg k_n \tag{5}$$

By plotting the left side in the equation versus lg *t*, we can get a straight line. The *n* (the slope of the straight line) and k_n (the intersection) values can also be obtained.

The relative amount of crystallinity for iPP and the blends have been plotted in Fig. 2 for 118 and 130 °C. All curves in Fig. 2 show a sigmoidal shape, indicating a fast primary process during the initial stages and slower secondary process during the later stages. As can be seen, Fig. 2 shows that the blends crystallize faster than

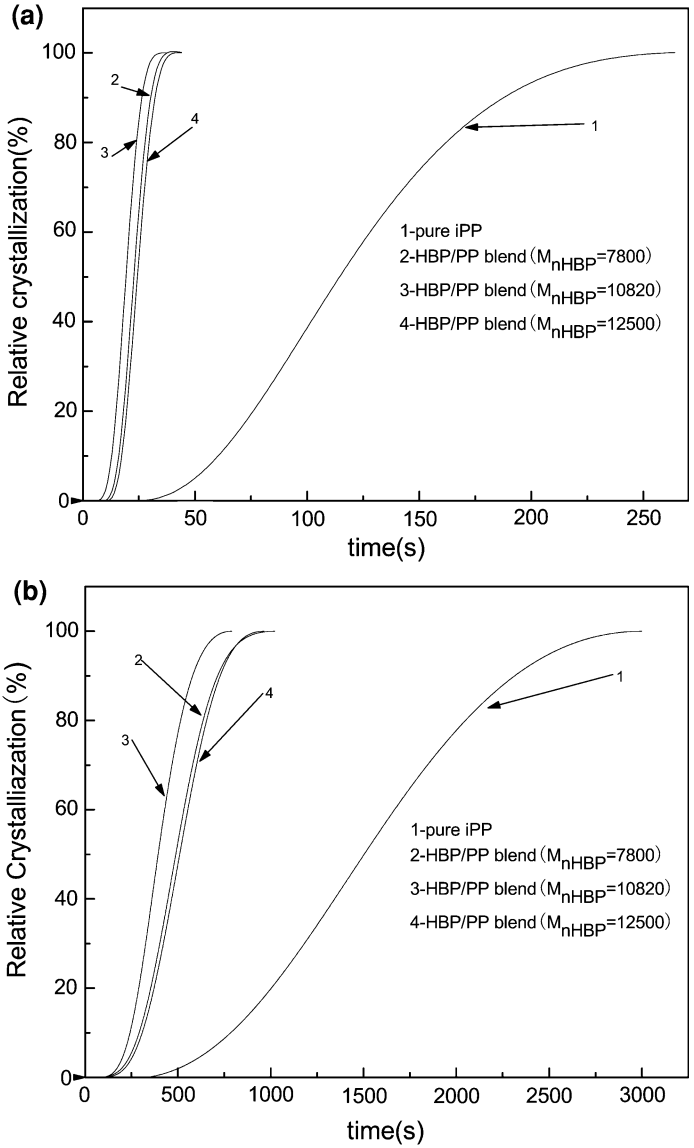

Fig. 2 Development of relative crystallinity with time for isothermal crystallization for iPP and 5% HBP/PP blends. **a** 118 °C **b** 130 °C

iPP remarkably. Moreover, the crystallization rate increases with increasing the HBP molecular weight in blends, however, the crystallization rate of the blend decreases when the HBP ($\bar{M}_n = 12{,}500$) is added.

Plots of $\lg[-\ln(1 - X(t))]$ versus $\lg t$ are shown in Fig. 3. There are good linearities of $\lg[-\ln(1 - X(t))]$ versus $\lg t$ in a wide relative crystallinity range. It is clear that the Avrami equation is effective for analyzing the experimental data of the isothermal

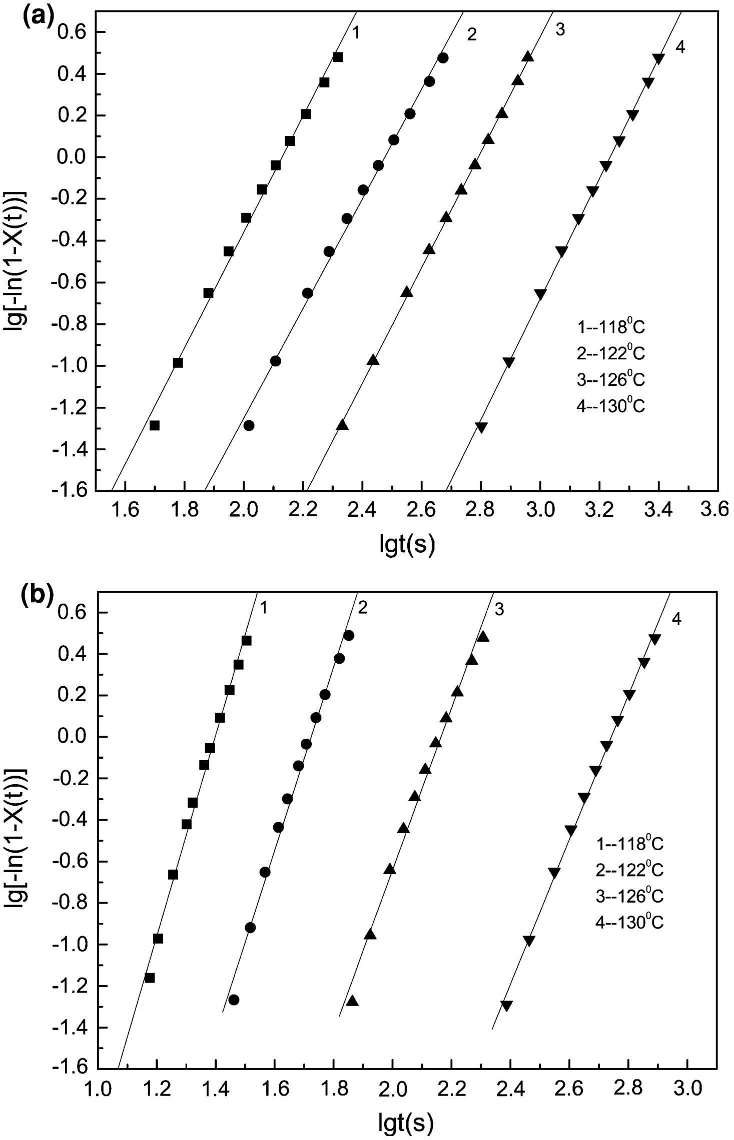

Fig. 3 Avrami plots for isothermal crystallization of iPP and HBP/PP blend at various crystallization temperatures. **a** iPP **b** HBP/PP blend ($\bar{M}_{n\text{HBP}} = 7{,}800$)

crystallization kinetics. The values of K_n, n, and $t_{½}$, obtained from Fig. 3 are listed in Table 1. As can be seen, $t_{½}$ of all samples increases with increasing crystallization temperature in agreement with earlier observations [10, 15]. The half time of pure iPP crystallization increases with the crystallization temperature, but at a much slower rate compared to the blends. This means that the dependence of crystallization kinetics on the crystallization temperature is much weaker for iPP than for HBP/PP blends.

The values of $t_{½}$ obtained from the experimental data are also given in Table 1. They are consistent with those calculated from Eq. 3, indicating the validity of the Avrami equation in this study. As can be seen, the order of values of $t_{½}$ is the same as the above. Furthermore, in the blends, the variety trend of the crystallization rate is the same as the above. The possible explanation is that a large number of polar branched chains coming from HBP act as nucleating agent, promoting the nucleation. Additionally, HBP may act as a lubricating agent, which resulted from approximately spherical molecular shape and the absence of chain entanglement, leading to a decrease in viscosity in blend, the diffusion of crystallizable chain segments towards the growing nuclei is facilitated, therefore, the crystallization rate increases remarkably. At the same time, interactions such as hydrogen bonding between polar groups of branching chains become stronger with increasing the HBP molecular weight, resulting a physically cross-linked network in the system, consequently, chain diffusion and mobility of the crystallizable segments diminish, and thus the crystallization process is slowed when the 5% HBP ($\bar{M}_n = 12{,}500$) is added in the blend.

Table 1 The various parameters of samples from the Avrami equation

Samples (HBP molecular weight)	T(°C)	n	lg k_n	$T^{a}_{½}$(s)	$t^{b}_{½}$(s)
Pure iPP	118	2.78	−5.912	114.87	117.76
	122	2.63	−6.511	254.27	259.21
	126	2.77	−7.725	543.39	538.55
	130	2.89	−9.357	1511.41	1522.00
$\bar{M}_n = 7{,}800$	118	4.86	−6.792	24.03	23.25
	122	4.41	−7.607	50.24	49.05
	126	3.90	−8.435	131.49	131.40
	130	3.48	−9.541	493.21	493.00
$\bar{M}_n = 10{,}820$	118	4.30	−5.718	18.94	19.73
	122	4.26	−6.945	40.39	39.32
	126	3.61	−7.406	100.44	101.71
	130	3.59	−9.510	398.53	406.31
$\bar{M}_n = 12{,}500$	118	5.01	−7.144	24.90	24.94
	122	4.73	−8.143	48.49	48.37
	126	3.99	−8.602	129.75	131.56
	130	3.63	−10.014	512.43	512.92

[a] Obtained from experimental data

[b] Calculated from Eq. 3

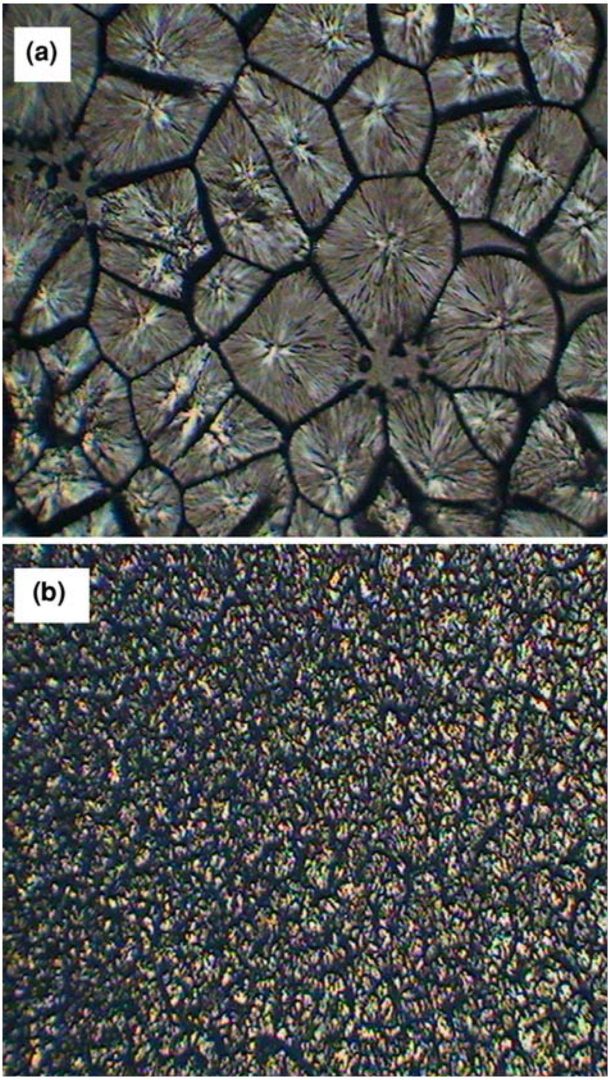

Fig. 4 The polarized micrographs of iPP and HBP/PP blend at 130 °C (magnification × 100). **a** iPP **b** HBP/PP blend ($\bar{M}_{n\mathrm{HBP}} = 12{,}500$)

Depending on the mechanism of nucleation and crystal growth, n should have different integer values. However, the non-integer values of the Avrami exponent are obtained for all the samples from experimental data, ranging from 2.78 to 5.01 and from 2.89 to 3.63 at the crystallization temperature, 118 and 130 °C, respectively. The deviation is likely attributed to secondary crystallization process, complex nucleation modes and the change in material density. Moreover, some experimental errors introduced in the determination of the zero point of crystallization also lead to non-integer value of n. The variation of n can be neglected within the error range in this study. An increase in the Avrami exponent means the addition of HBP influences the mechanism of nucleation and the growth of PP crystallites, one possible reason is usually attributed in the literature to a change from instantaneous to sporadic nucleation [11, 16]. Additionally, the fractal structure of hyperbranched polymer may have an influence on the growth of iPP crystallites and the diffusional mode of crystallizable segments towards the growing nuclei.

The intercept value (lg k_n) decreases with increasing crystallization temperature, which means a decrease in the nucleation rate constant and in the growth constant.

Figure 4 shows the polarized micrographs of iPP and HBP/PP blend ($\bar{M}_n = 12{,}500$) at 130 °C. The HBP/PP blend ($\bar{M}_n = 12{,}500$) shows the number of effective nuclei increases obviously and the spherulite size reduces rapidly, this indicates that HBP acts as a nucleating agent in the iPP phase. This result also provides the evidence that crystallization of the blend proceeds mainly via heterogeneous nucleation.

Conclusions

In this paper, we investigated the isothermal crystallization kinetics of pure isotactic polypropylene (iPP) and iPP with 5% AB_3 hyperbranched polymer (HBP) added using DSC. The Avrami equation was used to analyze the isothermal crystallization of samples. The results showed that the HBP acted as a heterogeneous nucleating agent and a lubricating agent during the crystallization of the blend and accelerated the crystallization rate remarkably. The value of $t_{1/2}$ became smaller with increasing the HBP molecular weight, however, the crystallization rate of the blend decreased when the HBP ($\bar{M}_n = 12{,}500$) was added. The polarized micrographs showed the number of effective nuclei increased obviously in HBP/PP blend. An increase in the Avrami exponent may be attributed to the fractal structure of hyperbranched polymer.

References

1. Mikhaylova Y, Dutschk V, M̈uller M, Grundke K, Eichhorn KJ, Voit B (2007) Study of the solid–liquid interface of hydroxyl-terminated hyperbranched aromatic polyesters (HBP-OH) in aqueous media II. Adsorption of model proteins. Colloids Surf A Physicochem Eng Asp 297:19
2. Wang X, Lai G, Jiang Z, Zhang Y (2006) Synthesis of water-soluble hyperbranched polymer and its application in acrylic latex. Eur Polym J 42:286
3. Thomasson D, Boisson F, Girard-Reydet E, Méchin F (2006) Hydroxylated hyperbranched polyesters as crosslinking agents for polyurethane networks: partial modification of the OH chain ends. React Funct Polym 66:1462
4. Pedrón S, Bosch P, Peinado C (2008) Using hyperbranched macromers as crosslinkers of methacrylic networks prepared by photopolymerization. J Photochem Photobiol A Chem 200:126
5. Marty J-D, Martinez-Aripe E, Mingotaud A-F, Mingotaud C (2008) Hyperbranched polyamidoamine as stabilizer for catalytically active nanoparticles in water. J Colloid Interface Sci 326:51

6. Yang J-P, Chen Z-K, Yang G, Fu S-Y, Lin Ye Y (2008) Simultaneous improvements in the cryogenic tensile strength, ductility and impact strength of epoxy resins by a hyperbranched polymer. Polymer 49:3168
7. Mo Z, Niu G, Chen H, Wu Y (2008) Synthesis and characterization of hyperbranched poly(amine-ester)/lanthanum/montmorillonite nanocomposites. Mater Lett 62:2043–2046
8. Burkinshaw SM, Froehling PE, Mignanelli M (2002) The effect of hyperbranched polymers on the dyeing of polypropylene fibres. Dyes Pigments 53:229
9. Wang SJ, Ba XW, Zhao BH, Zhang SW, Hou WL (2004) Synthesis and polymerization kinetics of AB_3 type hyperbranched poly(amide-estr)s. Acta Polym Sin 5:634
10. Varga J (1995) Polypropylene. In: Karger-Kocsis J (ed) Structure, blends and composites, chap. 3. Chapman and Hall, London, pp 56–115
11. Galeski A (1995) Polypropylene. In: Karger-Kocsis J (ed) Structure, blends and composites, chap. 4. Chapman and Hall, London, pp 116–139
12. Avrami M (1939) Kinetics of phase change. I. General theory. J Chem Phys 7:1103
13. Avrami M (1941) Kinetics of phase change. III. Granulation, phase change, and microstructure. J Chem Phys 9:117
14. Grenier D, Prud'homme RE (1980) Avrami analysis: three experimental limiting factors. J Polym Sci Polym Phys Ed 18:1655
15. Martuscelli E, Pracella M, Volpe GD, Greco P (1984) Morphology, crystallization and thermal behavior of isotactic polypropylene/low-density polyethylene blends. Makromol Chem 185:1041
16. Pratt CF, Hobbs SY (1976) Comparative study of crystallization rates by d. s. c. and depolarization microscopy. Polymer 17:12